

How to Cite:

Mohammed, S. H., & Hadi, N. J. (2022). Numerical approach for enhanced oil recovery with polymer flooding using CMG-STARS program. *International Journal of Health Sciences*, 6(S8), 2503–2516. <https://doi.org/10.53730/ijhs.v6nS8.12485>

Numerical approach for enhanced oil recovery with polymer flooding using CMG-STARS program

Saja Haider Mohammed

Department of Chemical Engineering and Petroleum Industries / Al-Mustaqbal University College, 51001, Hilla, Babil, Iraq
Corresponding author email: saja.haider@mustaqbal-college.edu.iq

Nizar Jawad Hadi

Department of Polymer and Petrochemical industries, Collage of Materials Engineering / University of Babylon /Iraq
Email: nizarjawadhadi@yahoo.com

Abstract---The polymer recovery efficiency of cationic polyacrylamide (PAM) has been evaluated for use as polymer flooding in the Basra oil reservoir. Initially, rheological, physical and petro physical were studied. Additionally, the polymer flooding core flooding experiment has been tested to see how well PAM solutions can be recovered. The comparative study between experimental and numerical study for PAM solution has been accomplished in terms of rheological properties, relative permeability curve and oil production. The results showed that PAM solution exhibit shear thinning effect which can efficiently improve the macroscopic sweep efficiency as well as microscopic displacement efficiency, and viscosity increase with high concentration. The overall recovery efficiency of 94.61 % from sandstone was determined for 2500_{ppm} PAM flooding. By contrast, brine water flooding was found to be 47.76%, showing that it was less effective than PAM solution. Cost analysis is another factor that affects a project's success. To support the experimental results, a simulation by the Computer Modelling Group (CMG) study has also been conducted.

Keywords---rheology, surface tension, interfacial tension, core flooding, computer modeling group (CMG), polymer flooding.

Introduction

Over the past half-century, polymer flooding has been a widely used approach for chemical enhanced oil recovery (CEOR) [1,2]. It was initially designed because of poor mobility ratios due to reservoir heterogeneity and/or high oil viscosity[3]. Polymers have been added to the water to improve the efficiency of both the aerial and volumetric sweep[4]. Polymer flooding is primarily a sweep augmentation method that reduces viscous fingering in order to improve cross flow between vertical heterogeneous layers[5,6]. To further improve microscopic displacement efficiency and reduce oil saturation during a water flood, non-Newtonian polymer solutions may be used. Any reservoir flooding application must take into account the injectivity of the water [7-9]. Whether injectivity can be accurately estimated within a reasonable error margin is an important factor in determining whether or not a project is financially viable[10].It is considerably more critical in polymer flooding applications because of the polymer's high viscosity and non-Newtonian behaviour. Formation fracture conditions may be reached if this behaviour persists, which could have a major impact on in-situ polymer rheology[11-13]. The discrepancy between field injectivity measurements and expectations has been explained in part by a slew of noteworthy discoveries in recent years. At far higher speeds, shear thickening takes place in radial flow [14] than in linear flow. Radial flow showed higher shear thinning than linear flow [15]. Polymers' in-situ rheology can also be significantly affected by the presence of residual oil [16]. Reduced in situ viscosity of a polymer with residual oil compared to when it does not have residual oil. The polymer's injectivity can be improved by reducing its elastic properties while retaining its viscous ones through preshearing it before to injection [17-20], which reduces or eliminates the extensional shear thickening behavior towards the well bore. Analysis of the results of polymer flood laboratory experiments and fundamental theory is greatly aided by numerical simulation [21]. A polymer field initiative's strategic planning is also vital for predicting its future performance and consequences [22]. Polymer flooding's relative permeability curves help reservoir rock two-phase flow behavior be better understood in the prediction of crude oil production, numerical simulation, and reservoir engineering [23].The extraction of crude oil is made more difficult by the high rate of water loss that occurs in the late phases of oilfield development [24]. As a result, crude oil recovery is boosted. Because of its effectiveness in reducing water cuts with improving oil output, polymer flooding technology has recently been adopted in France, China, the United States, and Canada. [25] Late-stage development for water-flooding oilfields with a high water cut has included polymer flooding, mainly in China [26]. It was shown that raising the viscosity of a polymer decreased the water relative permeability curve but had There is no influence on the oil relative permeability curve [27]. According to a study of the relative permeability curves, polymer flooding can also result in an increase in water saturation that is irreversible. Polymer injections have more complex physicochemical properties than water injections, such as rheology and residual resistance as well as adsorption and diffusion [28,29]. Thus, standard experiments cannot be utilized to study the impact of polymer solution physicochemical variables on relative permeability curves. The traditional approach for estimating polymer floods' relative permeability curves has been updated by several researchers, however only a portion of the polymer solution's properties can be taken into account[30]. Modeling polymer flooding in any

reservoir began with a three-dimensional numerical simulation, but this model did not include non-Newtonian polymer behavior in situ, which was later found to be crucial for the mechanisms of polymer flooding [31]. Modifying the Blake-Kozeny power law for fluids to account for additional properties such as reduced permeability and non-linear mixing of polymer and water, the effect of polymers on in-situ rheology was calculated [32]. The Darcy equation in radial flow and a mechanical degradation correlation were incorporated into an analytical model for infectivity in radial coordinates in order to compute the total injection pressure decrease [33]. This model was created to reproduce the decrease in polymer injectivity that was seen in laboratory and field research. It looked at the effect of polymer adsorption/retention on viscoelastic polymer rheology on deep-bed filtration and the formation of external filter cakes. According to [34], precise gridding is necessary to minimise velocity computation errors around the wellbore and thus more correctly capture polymer rheology. Polymer flooding modelling is included in commercial reservoir simulation software such as STARS by Computer Modeling Group Ltd. (CMG), ECLIPSE 100 by Schlumberger, and reveal by Petroleum Experts [35]. In this work field polymer injectivity studies will be improved by applying numerical simulations of polymer flooding at both laboratory and field sizes in this research. It's time to investigate the relationship between injection pressure and polymer rheology.

Experimental part

Materials and Methods

Polyacrylamide (PAM) with molecular weight ≥ 3000000 (g/mol), density (1.182) g/mol and glass transition temperature (159) $^{\circ}\text{C}$ provided from (china). Tap water, brine water and crude oil with viscosity (3.115) Cp and density (0.9993) g/cm^3 at 25°C were used. Rock (core) in type of sandstone provide from Nasiriya reservoir cut from depth of (2010.07) m.

Polymer Aqueous Solution

Brine water was prepared by mixing 20% of NaCl with tap water using magnetic stirrer for 10min. Mixing each (1000, 1500, 2000 and 2500) ppm of PAM with (50) ml tap water and brine water separately. Magnetic stirrer also, used for 30 min at 25°C to dissolve PAM added. The tests done after one day.

Polymer Aqueous Solution Characterization

Brookfield cone - plate viscometer with spindle: 41Z was used to measure rheological properties at different concentrations of polyacrylamide with tap and brine water. Viscosity test due to different shear rate (5-15) S^{-1} . The viscosity measurements were fitted by power law model given below:

$$\eta = K\dot{\gamma}^{n-1} \dots\dots\dots (1)$$

Here, η is shear viscosity (cP), K is consistency index ($\text{Cp}\cdot\text{s}^{n-1}$), $\dot{\gamma}$ is shear rate (S^{-1}), and n is the flow behavior index (dimensionless). Density test was performed using GP-120 S based on ASTM D-792 from China. The test made with different solutions. PH was perform using WTW, type Inolab 720. Technical Specification: 4X Alkaline AA, 1,5V. PH range: 2.000 to 19.99. Temperature: -5 to 105

C°. Surface tension and interfacial tension (IFT) was performed using JZYW-200B Automatic Interface Tensiometer provided through BEING UNITED TEST CO., LTD China. Check surface tension of polymer aqueous solutions in tap and brine water at 25°C are made in contact with air.

Relative Permeability Measurement

To determine the relative permeability of two-phase fluid in sandstone core, polymer core flooding experiments were undertaken utilizing Cationic polyacrylamide.

1. Core was cleaned by toluene and methanol, placed the core in a drying oven for 12 hours to dry it at 100 °C, saturated dried core by brine water, weight after and before saturated, put inside accumulative filled by brine water and weighted again. The volume of saturated water was used to calculate the porosity of the core.
2. Brine was injected into the core at various rates, and pressure drops across the core were measured. Darcy's law was used to calculate the brine permeability of cores.
3. After determining the brine permeability in 2, 2500ppm PAM/brine water was injected into the core at a flow rate of 6 cc/min until the pressure drop was stable, the post-polymer brine permeability was determined by repeating step 2. A relationship between Darcy velocity and flow rate is characterized by the following formula:

$$V_D = \frac{F_v}{A} \dots \dots \dots (2)$$

where F_v is the rate of flow, V_D is the Darcy velocity, and A is the core's cross-sectional area.

4. Following a determination of brine permeability in Step 2, a core was saturated with crude oil. Aside from the pressure drop across the core, the volume of brine water produced could be calculated when no brine water was created. A volume of saturated and generated brine water were used to compute the irreducible water saturation. Absolute permeability, as defined by Darcy's law, refers to oil permeability at irreducible water saturation.
5. As depicted in Figure 1, experiments were carried out with brine water and polymer flooding separately at a predetermined injection rate after Step 4. The total amount of oil and water produced over time, as well as the injection pressure, was recorded. The experiment was halted when no more oil was produced. The saturated and produced oil quantities were used to estimate the remaining oil saturation. The findings are summarised in Tables 3 and 4.

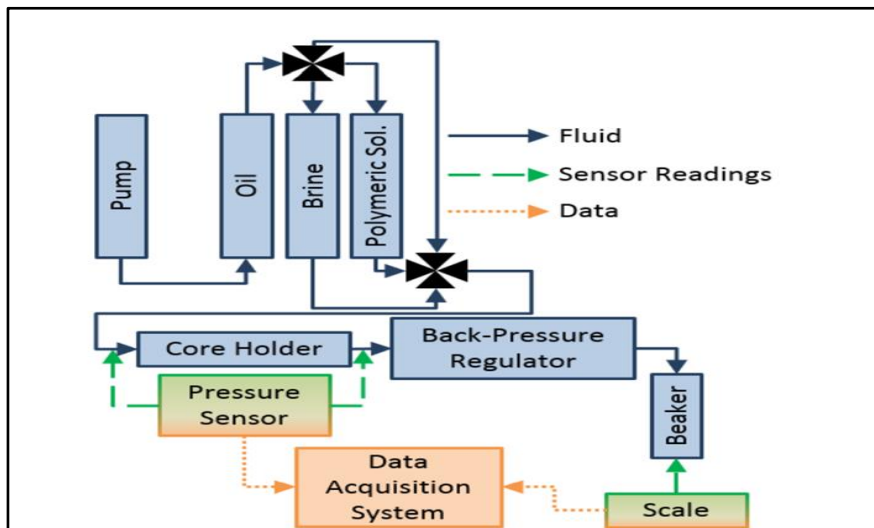


Figure 1 Core Flooding Test [36]

Simulation Methodology

Main Assumption

1. Initially, the reservoir is composed of two phases: crude oil and brine water or polymer flooding.
2. In the basic model, the amount of free gas/solvent gas is assumed to be zero.
3. A grid-based core model with homogeneous characteristics and no geological complexities/heterogeneities is considered.
4. Radial fluid flow is minor in comparison to axial fluid flow.
5. No chemical reactions take place.
6. Oil, brine water, or polymer flooding obeys Darcy's Law when it flows through porous medium.

Table 1 Rock Properties

| Rock Properties | Values |
|---------------------------|-----------|
| Diameter , cm | 3.8 |
| Length, cm | 5.7 |
| Permeability | 69 |
| Porosity, \emptyset % | 38 |
| Pressure, Psi | 345 |
| Temperature, $^{\circ}$ C | 25 |
| Rock Type | sandstone |

Building

The CMG-STARS tool was used to simulate the core flooding experiment with the polymer solution, and the CMG-CMOST tool was used to perform automated history matching. The cylindrical core was modeled with the same core length and diameter as shown in Table 1. The porosity and permeability for the model's rock

properties were assigned based on the results of the core flooding experiment. The fluid properties for the model, including the viscosity of brine, crude oil, and polymer solutions, were determined as described in the preceding sections. The relative permeability data endpoints were chosen as variables to be varied for the history matching of the simulated and experimental results.

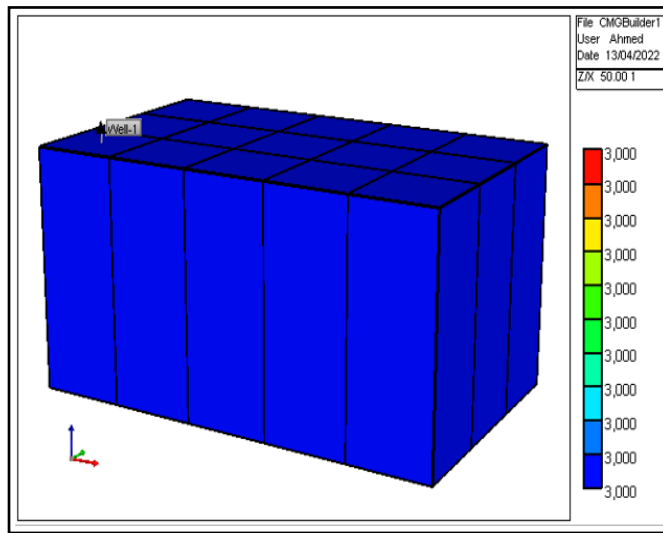


Figure 2 Cartesian grid (centroid X) pattern for flooding simulation.

Result and Discussion

Viscosity Curve

This subsection included four experimental cases as appear in figure 3, viscosity curve behavior of (1000, 1500, 2000 and 2500) ppm at 25°C. Tap and brine water behave as Newtonian flow without mixing with Cationic PAM polymer. Which independent of shear rate. While the non-Newtonian behavior and shear thinning effects increase with the PAM concentrations increasing. The shear viscosity indicates rapid decreasing up to 100 S^{-1} shear rate then the behavior gradually decreasing and attempt to be stable. Shear viscosity increases with PAM concentration increasing. Gel like formation increase with PAM concentration increasing which decreases mobility ratio. While the viscous finger reduces by increasing the viscosity of PAM aqueous solution [37]. These results compatible with the boundary conditions of reservoir [38].

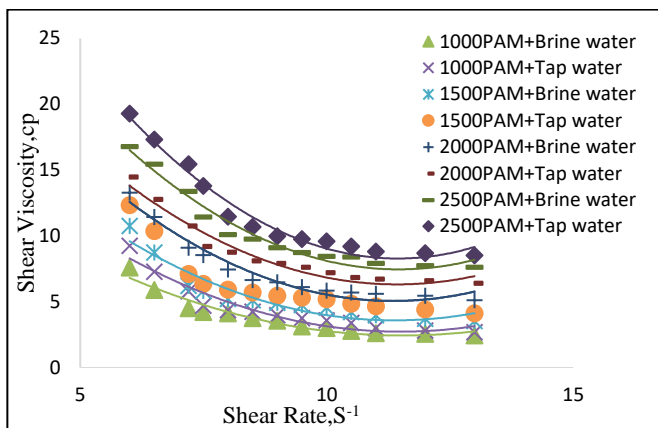


Figure 3 Shear viscosity versus shear rate for different PAM aqueous solutions

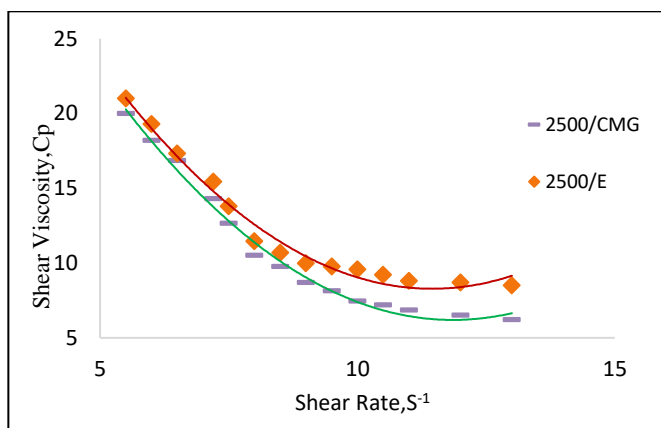


Figure 4 Shear viscosity vs. shear rate of 2500 ppm pam/brine water

Shown in Figure 4 is: We can demonstrate convergence between experimental and numerical studies by comparing the two. Furthermore, it shows that the polymer solution has significant shear thinning rheological capabilities. As shear rate rises, so does the polymer solution's viscosity. Because polymer molecules become more entangled at higher shear rates, the hydrodynamic radius and viscosity of the polymer solution drop, resulting in a decrease in shear thinning [39].

Density

Density of polymer aqueous solution increase with (1000, 1500, 2000 and 2500) ppm PAM increasing respectively as show in table 1. High density referred by increase interlink ages between chains. On the other hand dissolved these concentrations by brine water led to lower density compared with the tap water.

PH

Dissolved (1000, 1500, 2000 and 2500) ppm PAM respectively in water increase PH value from neutral to basic with same magnitude for all concentrations. On the other hand, when dissolved these concentrations by brine maintained on constant PH values with same concentrations as show in table2.The PAM/ brine aqueous solutions indicate higher PH values than that with tap water.

Table 2 Fluid Properties

| Aqueous Solution (ppm) | Density (g/cm ³) | PH | Surface Tension (Mn/m) | Interfacial Tension (Mn/m) | Power Law Index (n) | Consistency K (Pa .s ²) |
|------------------------|------------------------------|----|------------------------|----------------------------|---------------------|-------------------------------------|
| oil | 0.9993 | 10 | 35 | - | - | - |
| Brine water | 0.65 | 9 | 20 | 15 | - | - |
| 1000PAM/ tap water | 0.98 | 8 | 25.8 | 9.2 | 0.3283 | 0.08544 |
| 1500 PAM/ tap water | 0.9838 | 8 | 26.6 | 8.4 | 0.2731 | 0.1308 |
| 2000 PAM/ tap water | 0.9952 | 8 | 27.3 | 7.7 | 0.2358 | 0.23003 |
| 2500 PAM/ tap water | 0.9979 | 8 | 28.5 | 6.5 | 0.1434 | 0.4783 |
| 1000PAM/ brine water | 0.9791 | 9 | 25.1 | 9.9 | 0.4657 | 0.03837 |
| 1500 PAM/ brine water | 0.9799 | 9 | 25.5 | 9.5 | 0.3593 | 0.08093 |
| 2000 PAM/ brine water | 0.9951 | 9 | 26.8 | 8.2 | 0.2630 | 0.1746 |
| 2500 PAM/ brine water | 0.9968 | 9 | 27.7 | 7.3 | 0.1841 | 0.3521 |

Surface Tension and Interfacial Tension

The surface tension increases with the PAM concentration increasing for all solution. While the surface tension of PAM with tap indicate, higher value compared with brine water as show in table 1.The maximum surface tension values obtained for tap and brine aqueous solutions with 2500 ppm tables1 show that. The power low index n decreases and viscosity consequences K increase with the PAM concentrations increasing for tap and brine solutions. Calculated values for n and K comparable with the non- Newtonian flow behavior and shear thinning effect of PAM aqueous solution. The lower n value the higher shear thinning effect which representing by 2500ppm PAM aqueous solutions.

The IFT values for the polymer solution are presented in Table 2. According to the results, the addition different PAM concentration reduced oil-polymer IFT respectively from upper to lower. Then 2500 ppm PAM/brine water given lower IFT. By altering the wettability of porous media and lowering the IFT between oil and brine, polymer solutions can improve oil recovery. Reduced IFT reduces the capillary forces acting on oil trapped in pores, which enhances recovery [40]. Wettability of porous media regulates fluid distribution and flow inside a reservoir, which has a direct effect on oil recovery. This is a well-accepted fact. Nonetheless, the porous media's wettability leads in excellent recovery in a wet system [41].

Table 3 Petro physical Properties

| Core | Porosity (%) | Pore Volume (PV)% | Permeability (mD) | | |
|-----------|--------------|-------------------|-------------------|-------|------|
| | | | Ka | Kl | Ko |
| Sandstone | 24 | 13.24 | 69 | 62.04 | 43.4 |

Relative Permeability Curve

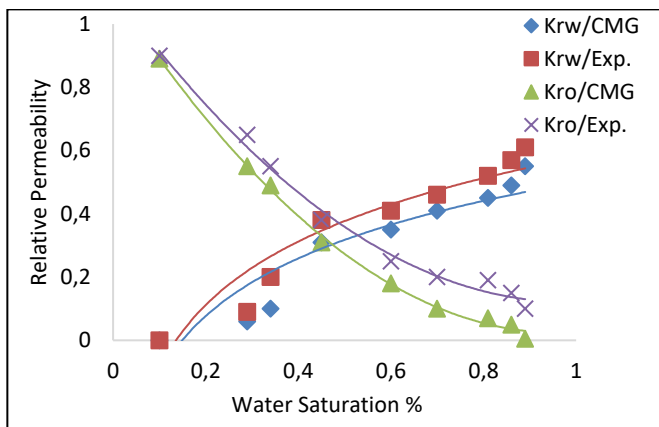


Figure 5 Relative permeability curve with water saturation for water flooding

Figure 5, when water flooding is injected in sandstone core. The cross point of water relative permeability (k_{rw}) with relative permeability of oil (k_{ro}) appear less than 0.5. This occurs because the mobility ratio, M , for water is expected to be greater than one, indicating the presence of viscous fingering. The formation is confirmed to be oil-wet based on earlier justifications. This means that capillary forces limit water floods. The oil is stuck to the rock surface, and this adhesion forces water to flow backwards through the pores. Additionally, the oil contained within the reservoir has a very high viscosity. This causes the water to finger through the oil and trickle through the pores' center [42].

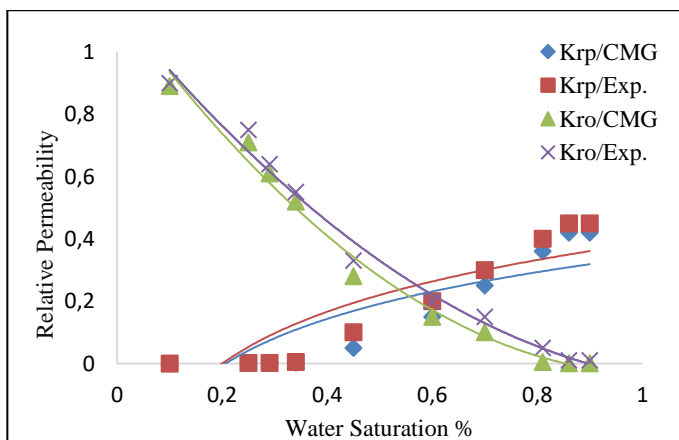


Figure 6 Relative permeability with water saturation for polymer flooding

Figure 6, represent comparison between experimental and modelling study by CMG program. From this figure we show the degree of convergence between experimental and modelling study. Additionally, all of these cases had a flow rate of 6cc/sec. The fundamental parameters for the core flooding experiments are listed in Tables 2 and 3. Water relative permeability (k_{rw}) and oil relative permeability (k_{ro}) intersect at a value less than 0.5, indicating that the mobility ratio is less than one and the polymer solution wets the porous media surface. Figure 6 depicts a wet reservoir in which the 2500ppm PAM/brine water is an excellent candidate for chemical tertiary recovery [43,44]. The actual core's circular cross-section was turned into a square cross-section with the same cross-sectional area (Figure2) and grid sizes of 2.22 cm along the y- and z-axes to aid in the development of a numerical simulation model of core flooding. The minimum bottom hole pressure in the numerical simulation model was set to 345 Psi since the production end was exposed to the atmosphere during core flooding.

Table 4 Oil Recovery

| Core | Solutions | Oil Recovery | Additional oil Recovery | Saturation% | | |
|------------|--------------------------|--------------|-------------------------|-------------|-----|------|
| | | | | Swi | Soi | Soi |
| | Brine water | 47.67 | - | | | 49.7 |
| Sands tone | 2500 ppmPAM /brine water | 94.61 | 47 | 9 | 91 | 5.39 |

Conclusion

1. Polymer flooding is a promising technique for chemical EOR. This is because, as compared to brine water flooding, it has been demonstrated to boost cumulative oil output.
2. Using a cone-plate viscometer, researchers were able to detect the flow of polymer solution in bulk and porous media, as well as the shear thinning behaviour at low shear rates.
3. As the PAM concentration increases, the power law index n decreases and the viscosity consistency K increases.
4. As PAM concentrations grew, density, surface tension, and oil recovery increased, whereas IFT decreased.
5. The relative permeability curves for brine water and polymer solution contain oil wet and water wet components, respectively. This conclusion is supported by experimental data from CMG-STARS.
6. The impacts of oil displacement efficiency were investigated using core flooding tests, which demonstrate that flooding with 2500ppm PAM/brine water performs significantly better than flooding with brine water alone.
7. good validation by CMG-STARS for rheological and relative permeability.
8. These studies in the context of the Basra oil reservoir could pave the way for future work.

Acknowledgments

The authors like to express their gratitude to Al-Mustaqbal University College/Department of Chemical Engineering and Petroleum Industries and University of Babylon/Department of Polymer and Petrochemical Industries, College of Materials Engineering for their collaborative efforts. Additionally, we would like to express our gratitude to everyone involved in the project.

References

1. Alfazazi, U., AlAmeri, W., & Hashmet, M. R. (2019). Experimental investigation of polymer flooding with low-salinity preconditioning of high temperature–high-salinity carbonate reservoir. *Journal of Petroleum Exploration and Production Technology*, 9(2), 1517-1530.
2. Alfazazi, U., Thomas, N. C., Alameri, W., & Al-Shalabi, E. W. (2020). Experimental investigation of polymer injectivity and retention under harsh carbonate reservoir conditions. *Journal of Petroleum Science and Engineering*, 192, 107262.
3. Alfazazi, U., Thomas, N. C., Alameri, W., & Al-Shalabi, E. W. (2020). Experimental investigation of polymer injectivity and retention under harsh carbonate reservoir conditions. *Journal of Petroleum Science and Engineering*, 192, 107262.
4. Al-Shakry, B., Skauge, T., Shaker Shiran, B., & Skauge, A. (2019). Polymer injectivity: Investigation of mechanical degradation of enhanced oil recovery polymers using in-situ rheology. *Energies*, 12(1), 49.
5. Alzaabi, M. A., Gausdal Jacobsen, J., Masalmeh, S., Al Sumaiti, A., Pettersen, Ø., & Skauge, A. (2020). Polymer injectivity test design using numerical simulation. *Polymers*, 12(4), 801.
6. Amirian, E., Dejam, M., & Chen, Z. (2018). Performance forecasting for polymer flooding in heavy oil reservoirs. *Fuel*, 216, 83-100.
7. Angu, K., Sharma, R., Alauddin, W., Bashir, M., & Aaghaz, S. (2022). Is there a correlation between heart rate recovery and androgen parameters in polycystic ovary syndrome? Heart rate recovery in polycystic ovary syndrome. *International Journal of Health Sciences*, 6(S1), 7014–7027. <https://doi.org/10.53730/ijhs.v6nS1.6508>
8. Azad, M. S., & Trivedi, J. J. (2019). Quantification of the viscoelastic effects during polymer flooding: a critical review. *SPE Journal*, 24(06), 2731-2757.
9. Bondor, P. L., Hirasaki, G. J., & Tham, M. J. (1972). Mathematical simulation of polymer flooding in complex reservoirs. *Society of Petroleum Engineers Journal*, 12(05), 369-382.
10. Cheraghian, G., & Hendraningrat, L. (2016). A review on applications of nanotechnology in the enhanced oil recovery part A: effects of nanoparticles on interfacial tension. *International Nano Letters*, 6(2), 129-138.
11. Corredor, L. M., Husein, M. M., & Maini, B. B. (2019). Impact of PAM-grafted nanoparticles on the performance of hydrolyzed polyacrylamide solutions for heavy oil recovery at different salinities. *Industrial & Engineering Chemistry Research*, 58(23), 9888-9899.
12. Davarpanah, A. (2020). Parametric study of polymer-nanoparticles-assisted injectivity performance for axisymmetric two-phase flow in EOR processes. *Nanomaterials*, 10(9), 1818.

13. Delamaide, E. (2019, June). How to use analytical tools to forecast injectivity in polymer floods. In SPE Europec featured at 81st EAGE Conference and Exhibition. OnePetro.
14. Druetta, P., Raffa, P., & Picchioni, F. (2019). Chemical enhanced oil recovery and the role of chemical product design. *Applied energy*, 252, 113480.
15. Du, Y., & Guan, L. (2004, November). Field-scale polymer flooding: lessons learnt and experiences gained during past 40 years. In SPE International Petroleum Conference in Mexico. OnePetro.
16. Farfán, R. F. M., Zambrano, T. Y. M., Badillo, F. R. A., & Solís, A. A. H. (2020). Design and construction of an industrial ship conditioning system. *International Journal of Physical Sciences and Engineering*, 4(1), 29–38. <https://doi.org/10.29332/ijpse.v4n1.423>
17. Ghomrassi-Barr, S., & Aliouche, D. (2016). A rheological study of xanthan polymer for enhanced oil recovery. *Journal of Macromolecular Science, Part B*, 55(8), 793-809.
18. Han, C. D. (2007). *Rheology and processing of polymeric materials: Volume 1: Polymer Rheology (Vol. 1)*. Oxford University Press on Demand.
19. Jamaloei, B., Kharrat, R., & Torabi, F. (2010, December). A mechanistic analysis of viscous fingering in low-tension polymer flooding in heavy-oil reservoirs. In SPE Latin American and Caribbean Petroleum Engineering Conference. OnePetro.
20. Jouenne, S. (2020). Polymer flooding in high temperature, high salinity conditions: Selection of polymer type and polymer chemistry, thermal stability. *Journal of Petroleum Science and Engineering*, 195, 107545.
21. Kaminsky, R. D., Wattenbarger, R. C., Szafranski, R. C., & Coutee, A. S. (2007, December). Guidelines for polymer flooding evaluation and development. In IPTC 2007: International Petroleum Technology Conference (pp. cp-147). European Association of Geoscientists & Engineers.
22. Lahalih, S. M., & Ghloum, E. F. (2010, June). Polymer compositions for sand consolidation in oil wells. In SPE Production and Operations Conference and Exhibition. OnePetro.
23. Laoroongroj, A., Gumpenberger, T., & Clemens, T. (2014, October). Polymer Flood Incremental Oil Recovery and Efficiency in Layered Reservoirs Including Non-Newtonian and Viscoelastic Effects. In SPE Annual Technical Conference and Exhibition. OnePetro.
24. Laoroongroj, A., Gumpenberger, T., & Clemens, T. (2014, October). Polymer Flood Incremental Oil Recovery and Efficiency in Layered Reservoirs Including Non-Newtonian and Viscoelastic Effects. In SPE Annual Technical Conference and Exhibition. OnePetro.
25. Leblanc, T., Braun, O., Thomas, A., Divers, T., Gaillard, N., & Favero, C. (2015, August). Rheological properties of stimuli-responsive polymers in solution to improve the salinity and temperature performances of polymer-based chemical enhanced oil recovery technologies. In SPE Asia Pacific Enhanced Oil Recovery Conference. OnePetro.
26. Li, Z., & Delshad, M. (2014). Development of an analytical injectivity model for non-Newtonian polymer solutions. *SPE Journal*, 19(03), 381-389.
27. Liu, Q., Shen, P., & Wu, Y. S. (2004). Characterizing two-phase flow relative permeabilities in chemical flooding using a pore-scale network model (No. LBNL-54750). Lawrence Berkeley National Lab.(LBNL), Berkeley, CA (United States).

28. Liu, Z., Li, Y., Lv, J., Li, B., & Chen, Y. (2017). Optimization of polymer flooding design in conglomerate reservoirs. *Journal of Petroleum Science and Engineering*, 152, 267-274.
29. Lomeland, F., Ebeltoft, E., & Thomas, W. H. (2005, August). A new versatile relative permeability correlation. In *International symposium of the society of core analysts*, Toronto, Canada (Vol. 112).
30. Lotfollahi, M., Farajzadeh, R., Delshad, M., Al-Abri, A. K., Wassing, B. M., Al-Mjeni, R., ... & Bedrikovetsky, P. (2016). Mechanistic simulation of polymer injectivity in field tests. *Spe Journal*, 21(04), 1178-1191.
31. Mandal, A. (2015). Chemical flood enhanced oil recovery: a review. *International Journal of Oil, Gas and Coal Technology*, 9(3), 241-264.
32. Nejad, K. S., Berg, E. A., & Ringen, J. K. (2011, September). Effect of oil viscosity on water/oil relative permeability. In *International symposium of the society of core analysts*, Austin, TX, USA.
33. Nilsson, M. A., Kulkarni, R., Gerberich, L., Hammond, R., Singh, R., Baumhoff, E., & Rothstein, J. P. (2013). Effect of fluid rheology on enhanced oil recovery in a microfluidic sandstone device. *Journal of non-newtonian fluid mechanics*, 202, 112-119.
34. Rellegadla, S., Prajapat, G., & Agrawal, A. (2017). Polymers for enhanced oil recovery: fundamentals and selection criteria. *Applied microbiology and biotechnology*, 101(11), 4387-4402.
35. Sarsenbekuly, B., Kang, W., Yang, H., Zhao, B., Aidarova, S., Yu, B., & Issakhov, M. (2017). Evaluation of rheological properties of a novel thermo-viscosifying functional polymer for enhanced oil recovery. *Colloids and Surfaces A: Physicochemical and Engineering Aspects*, 532, 405-410.
36. Seright, R. S. (1983). The effects of mechanical degradation and viscoelastic behavior on injectivity of polyacrylamide solutions. *Society of Petroleum Engineers Journal*, 23(03), 475-485.
37. Seright, R. S. (2010). Potential for polymer flooding reservoirs with viscous oils. *SPE Reservoir Evaluation & Engineering*, 13(04), 730-740.
38. Shakeel, M., Samanova, A., Pourafshary, P., & Hashmet, M. R. (2021). Capillary Desaturation Tendency of Hybrid Engineered Water-Based Chemical Enhanced Oil Recovery Methods. *Energies*, 14(14), 4368.
39. Skauge, A., & Salmo, I. (2015, April). Relative Permeability Functions for Tertiary Polymer Flooding. In *IOR 2015-18th European Symposium on Improved Oil Recovery* (pp. cp-445). European Association of Geoscientists & Engineers.
40. Skauge, A., Zamani, N., Gausdal Jacobsen, J., Shaker Shiran, B., Al-Shakry, B., & Skauge, T. (2018). Polymer flow in porous media: Relevance to enhanced oil recovery. *Colloids and Interfaces*, 2(3), 27.
41. Wang, C., Liu, P., Wang, Y., Yuan, Z., & Xu, Z. (2018). Experimental study of key effect factors and simulation on oil displacement efficiency for a novel modified polymer BD-HMHEC. *Scientific Reports*, 8(1), 1-9.
42. Wang, D., Li, C., & Seright, R. S. (2020). Laboratory Evaluation of Polymer Retention in a Heavy Oil Sand for a Polymer Flooding Application on Alaska's North Slope. *SPE Journal*, 25(04), 1842-1856.
43. Wang, L., Liu, C., Jiang, P., Zhang, H., Tian, X., Zhao, N., & Mahlalela, B. M. (2019). Characterization of two-phase flow in porous media using global mobility. *Journal of Petroleum Science and Engineering*, 177, 188-197.

44. Widana, I.K., Sumetri, N.W., Sutapa, I.K., Suryasa, W. (2021). Anthropometric measures for better cardiovascular and musculoskeletal health. *Computer Applications in Engineering Education*, 29(3), 550–561. <https://doi.org/10.1002/cae.22202>
45. Xin, X., Yu, G., Chen, Z., Wu, K., Dong, X., & Zhu, Z. (2018). Effect of non-newtonian flow on polymer flooding in heavy oil reservoirs. *Polymers*, 10(11), 1225.
46. Yadali Jamaloei, B., Kharrat, R., & Torabi, F. (2010). Analysis and correlations of viscous fingering in low-tension polymer flooding in heavy oil reservoirs. *Energy & fuels*, 24(12), 6384-6392.
47. Zhong, H., Zhang, W., Fu, J., Lu, J., & Yin, H. (2017). The performance of polymer flooding in heterogeneous type II reservoirs—An experimental and field investigation. *Energies*, 10(4), 454.